Nordic Hydrology, 30 (2), 1999, 81-108

Evaporation from Snow in the Central Sierra Nevada of California

Al Leydecker and John M. Melack

Dept. of Ecology, Evolution and Marine Biology, and the
Institute for Computational Earth System Science,
University of California, Santa Barbara, CA 93106

Evaporation from snow was calculated with the mean-profile method using single-level meteorological data at eight locations representing a variety of alpine and sub-alpine terrain in the central Sierra Nevada, California. Four to six years of data were analyzed at most of the sites. Evaporation from snow was highest in mid-winter, when the vapor pressure gradient between the snow surface and the air was at its maximum, and declined throughout the snowmelt season. Near the end of snowmelt, condensation of water vapor on the snow surface often matched or exceeded evaporative loss. Annual evaporation from the snowpack varied from 12 to 156 mm. We estimate mean annual regional evaporation in the sub-alpine and alpine zones (excluding evaporation from tree-captured snow and during wind re-deposition) as 80 to 100 mm, approximately 7 per cent of the maximum accumulation during an average snow year. Evaporation during snowmelt contributed only minor amounts to the total seasonal loss, typically around 25 mm, or about 2% of the maximum average accumulation.

Introduction

In 1934 Francois Matthes, referring to evaporation (as used herein, evaporation includes all of the processes by which water is transferred between the snow surface and atmosphere) from snow in alpine areas of the Sierra Nevada, stated: "(I've) been impressed again and again by the fact that strongly sunpitted snow fields above 12,000 feet waste away during the summer without contributing a drop of water to

the streams below ... It follows that these upper snow fields are in no sense the sources of streams and are to be excluded from any estimates of runoff based on snow surveys." In an experiment designed to test Matthes' conclusions, Robert Sharp (1951) located an isolated snow bank on bedrock (at 3,720 m on the eastern side of the Sierra Nevada), and after measuring its volume, installed a weir to record snowmelt. He noted, "These measurements showed that approximately 99 per cent of the wastage ran off through the weir, leaving about 1 per cent for evaporation and other losses ... These results strongly suggest that evaporation occupies a relatively minor part in the ablation of snow in areas above 12,000 feet." It would be difficult to find two more diametrically opposed conclusions; and the importance of evaporation from snow continues to be argued.

Previous energy-balance studies on melting snowpacks have usually found little evaporation, but a few drew the opposite conclusion (Table 1). About a third show a mass gain through condensation rather than evaporative loss. Measured evaporation varied widely, up to a maximum of 2.35 mm day^{-1}, and even the most recent studies reflect a wide disparity.

At Emerald Lake in the central Sierra Nevada, Marks and Dozier (1992) used mean-profile methods to calculate evaporation from snow at two sites during 1986. They reported a total loss of 451 mm at the lake outlet and 537 mm on an exposed ridge. Losses during snowmelt were 201 mm (9% of the snowpack) and 284 mm (13%), respectively. Kattelmann and Elder (1991) calculated total evaporation from snow as 18% in 1986, and 33% in 1987 (a drought year with a third of the previous year's snowpack and a shortened melt season). They concluded that, "approximately 80 per cent of the annual evaporative loss was from sublimation off of snow ... at rates of 1 to 2 mm of water per day, with higher values on dry, windy days."

Anderson (1976), summarizing work done at the Central Sierra Snow Laboratory (CSSL) near Lake Tahoe, California, reached a contrasting conclusion. Using similar mean-profile methodology, he calculated average evaporation rates of about 2 mm per month during the accumulation season, and 4 mm per month during snowmelt. While his study was conducted in forest clearings, where lower wind speeds account for some differences, the overall results were lower than those at Emerald Lake by a factor of more than 30.

Evaporation requires a vapor pressure difference between the surface and the overlying air, and wind generated turbulence. A third factor, atmospheric stability or instability, dampens or reinforces the upward flux of water vapor. High winds passing dry air over hot moist surfaces maximize evaporation. Winter conditions in the Sierra Nevada are not usually conducive to high rates of evaporation. Mild days, with temperatures often above freezing, produce low vapor pressure differences: typical mid-winter values are 1 to 2 mb. At night, lower temperatures further diminish the small differences and with snow-surface temperature usually lower than that of the air, stable atmospheric conditions often prevail. Only high winds or unusual conditions could account for high evaporation.

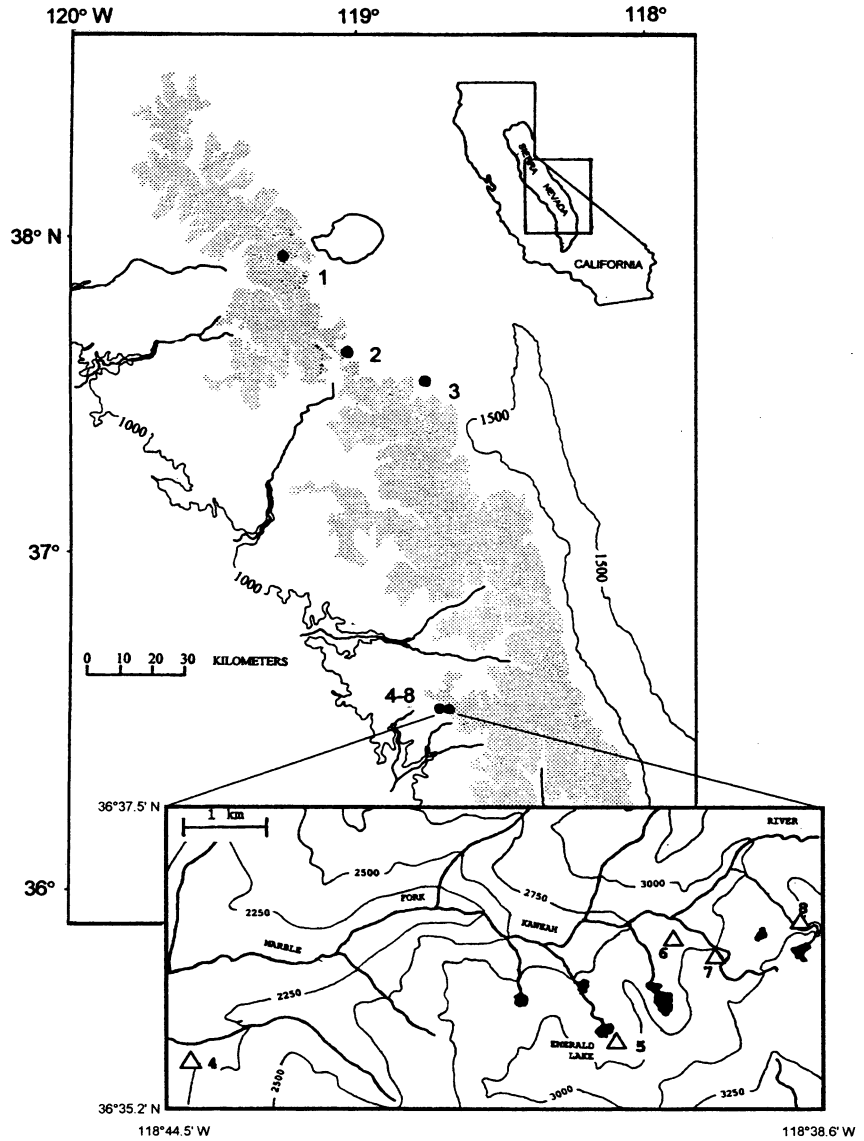

Fig. 1. Location map showing the meteorological stations used in the study: 1) Spuller, 2) Mammoth, 3) SNARL, 4) Wolverton, 5) Emerald, 6) Mini-catchments, 7) M1 and 8) M3. The shaded area represents elevations above 3,000 m (~timberline).

During snowmelt, atmospheric vapor pressures increase with rising temperature while the snow-surface is constrained to the saturation vapor pressure at 0°C. Stable atmospheric stratification becomes the norm. As the season progresses, atmospheric vapor pressure may exceed that of the snow-surface, producing condensation. High evaporation at this time seems improbable.

Table 1 – The relative utilization of energy between snowmelt and evaporation for a melting snow pack. Data from Kuusisto (1986, Table 1) and Pluss and Mazzoni (1994, Table 4). Negative values and "C" indicate condensation. Conversion factors used: 1 watt m^{-2} = 0.259 mm day^{-1} of snowmelt = 0.0305 mm day^{-1} of evaporation from snow or ice = 0.0345 mm day^{-1} of condensation from water vapor.

reference	location	elev.	time period	snowmelt		evaporation	
		m		%	mm day^{-1}	%	mm day^{-1}
Miller (1955)	open field (California) 37°N			82		18	
Gold & Williams (1960)	open field (Canada) 45°N	100	Mar 1959	26	7	74	2.35
Wendler (1967)	open field (Alaska) 67°N		Mar-Apr 1966	76		24	
Anderson (1968)	open field in mountains (California) 37°N		'47-'51 snow seasons	100		C	
			'47-'51 Apr-May	100		C	
Treidl (1970)	open field (Michigan) 46°N		Jan 23 1969	100	15	C	-0.72
Dewalle & Meiman (1971)	forest opening (Colorado) 39°N	3260	Jun 1968	97	50	3	0.18
Fohn (1973)	Peyto Glacier (Canada)	2510	15 days in May	100	47	C	-0.50
de la Casiniere (1974)	open field in mountains (France) 46°N	3550	July 1968	85	16	15	0.33
	open field in mountains (Spain) 41°N	1860	Apr 1970	47	10	42	1.05
	Mt. Blanc, French Alps	3550	23 days in July	81	5	19	0.15
Weller & Holmgren (1974)	open field (Alaska) 71°N	10	Jun 1971	49		10	
Granger & Male (1978)	open field in prairies (Canada) 51°N		'74 melt	84	8	10	0.11
			'75 melt	70	5	29	0.24
			'76 melt	82	3	14	0.07
Martin (1975)	St. Sorlin Glacier (France)	2700	11 days in summer	93	14	7	0.11
Hendrie & Price (1979)	deciduous forest (Ontario) 46°N		Apr 1978	100	10	0	0
Kuusisto (1979)	open field (Finland) 51°N	60	melt season '68-'73	96	7	4	0.03
Harstveit (1981)	open field in mountains (Norway) 60°N	435	Apr-May '79-80	100	12	0	0
			cloudy days	100	23	C	-0.80
			clear days	76	7	24	0.26

cont.

Table 1 – Continued.

reference	location	elev.	time period	snowmelt		evaporation	
		m		%	mm day^{-1}	%	mm day^{-1}
Braun & Zuidema (1982)	small basin, 23% forest (Switzerland) 47°N	800	high melt days'77-'80	100	23	C	-0.80
Eaton & Wendler (1981)	open field (Alaska) 65°N		April 1980	32	3	68	0.75
Kuusisto (1982)	open field (Finland) 61°N		high melt days'59-'78	100	14	C	-0.04
	open field 67°N		high melt days'59-'78	77	15	23	0.53
Prowse & Owens (1982)	open field in mountains (New Zealand) 43°S	1500	Oct-Nov '76-'80	100		C	
			rainy days	100		C	
			days with high heat	100		C	
Funk (1984)	Rhonegletscher, Swiss Alps		summer	99	44	1	0.06
Moore & Owens (1984)	open field in mountains (New Zealand) 43°S	1450	melt season 1982	100	31	C	-1.03
Aguado (1985)	open field (Wisconsin) 3 sites 43-45°N		melt seasons '53-'54	57		12	
Vehvilainen (1986)	small basin, 82% forest (Finland) 64°N	120	melt seasons '71-'81	87	5	13	0.09
Harding (1986)	Finse (Norway)	1000	15 days in May	100	12	C	-0.01
Calanca & Heuberger (1990)	Urumqi Glacier #1, Tien Shan (China)	3900		81	16	19	0.46
Marks & Dozier (1992)	Emerald Lake (California) 37°N	2800	May '86	43	11	57	1.65
			Jun '86	62	30	38	2.17
Pluss & Mazzoni (1994)	Swiss Alps	2600	18 days in May '92	97	10	3	0.03
Cline (1995)	Niwot Ridge (Colorado) 40°N	3520	melt season 1994	76	17	23	0.49

In a long-term study of the consequences of acidic precipitation on headwater catchments in the Sierra Nevada (Melack *et al.* 1997), we collected meteorological data, over periods varying from 2 months to 8 years, at 8 high elevation sites (Fig. 1). The mean-profile method, using meteorological measurements at a single-level, was used to calculate evaporation from snow at each location. In this paper we report the results, compare seasonal and inter-site differences, and discuss problems with the method and its sensitivity to our assumptions. By using locations that exemplify a wide variety of terrain, we attempt to evaluate the overall importance of evaporation from snow on the region's alpine and sub-alpine catchments (timberline is at 3,000 m).

Table 2 – Weather stations used in the study. Numbers in brackets refer to meteorological instruments installed (as listed in Table 3) and the above ground instrument heights at each station.

Site and Location	Description
Emerald 36°35.97'N, 118°40.20'W 2800 m	Located in a glacial cirque, behind (~80 m) and above (~20 m) the lake. The upslope fetch (in the direction of the prevailing winds) is good, but the fetch in other directions is marginal. The record begins in Sept. 1991 and has few gaps. [1 (at 5.5m), 4 (at 4.7m), 6 (at 6.1m), 8, 9 & 11; 2 & 7 at two additional levels in spring 1994 (1.8 and 3.3m)]
Mammoth 37°38.48'N, 119°01.78'W 2930 m	Located on a slightly sloping bench about half way up the flank of the mountain. The fetch is good in the direction of the prevailing wind and adequate for the other directions. The record begins in Sept. 1989 and is generally good, although there are a number of significant gaps. [2, 7, 7a, 8 (3 facing up, clear, red, thermal; 2 facing down, clear, red) & 10 (all at 7.9m)]
Mini-catchments 36°36.67'N, 118°39.71'W 2960 m	Located on a level and open ridge. The ridge is perpendicular to the direction of the predominant up-and-down canyon winds; the fetch is good in all directions with the exception of the southeast, where a small clump of trees formed an obstruction. In operation during the spring of 1992 and 1993. The record is good for the snowmelt season of 1993. [2, 7 (both at 5.8m), 7a, 8 (1 facing up; 1 facing down) & 10; 2 & 7 at an additional level in spring 1993 (2.5m)]
M1 36°36.55'N, 118°39.23'W 3090 m	Located on a north-facing slope, next to an outlet stream below a small pond. The undulating, slightly sloping, terrain is open and free of vegetation and the fetch is good in all directions. A record exists for May and June of 1994. [2 (at 3.7m) & 7 (at 4.6m)]

cont.

Table 2 – Continued.

Site and Location	Description
M3 36°36.68'N, 118°38.50'W 3250 m	Situated similar to M1, at a higher elevation in a flat and open area on the same plateau, with good fetch in all directions. The record exists for April through June of 1993. [2 (at 4.3m) & 7 (at 4.8m)]
SNARL 37°36.79'N, 118°49.83'W 2160 m	Located in Long Valley at the base of the eastern Sierra Nevada escarpment, on the glacial outwash plain~2 km from the mouth of Convict Canyon. The record begins in Oct. 1989 and is essentially complete. The area is level and the fetch is good for up-and-down canyon winds, adequate in other directions (some low shrubs to the south, and buildings to the north). [3 (at 2m), 5 (at 3.8m), 8 & 10]
Spuller 37°56.93'N, 119°16.91'W 3120 m	Located in a narrow canyon (100 m below the lake. The fetch for the prevailing wind direction (down canyon) is adequate, marginal for the other directions. The record begins in Oct. 1989, but little data are available for the early years. The latter record is better, but still has large gaps; only 1993 is substantially complete. [1 (at 5.5m), 4 (at 4.7m), 6 (at 6.1m), 8, 9 & 11]
Wolverton 36°35.74'N, 118°44.16'W 2190 m	Located in a forest clearing (~25 m in diameter) adjacent to a large meadow; a few scattered tall trees amid low younger growth (5 to 8m) form the surrounding stand. Although somewhat questionable as to fetch and instrument height, the openness of the stand should place the met instruments within the lower boundary layer. The record is excellent, providing almost continuous coverage from Nov. 1986. [2 (at 8.5m), 7 (at 9.5m), 7a, 8 & 11]

Meteorological Data

Brief descriptions of the weather stations used in the study, the station location, elevation, instrument heights and the length and quality of the data record, are given in Table 2. Table 3 describes the meteorological instruments installed at each station.

Mean-Profile Model

Methods for calculating turbulent energy fluxes, using short-term measurements of mean temperature, humidity and wind speed, are variously referred to as flux-profile, similarity, aerodynamic or mean-profile. We used equations from Brutsaert (1982) and the term "mean-profile." The equations, for meteorological data from a single-level and including corrections for atmospheric stability, are

Table 3 – Meteorological instruments used at the weather stations.

Parameter	no.	Description
Air Temperature	1	Omnidata ES 060 Thermistor: range, -50 to +80 °C; precision, ±0.25 °C; response time, 90 s; mounted in a EA 130V radiation shield.
Air Temperature and Humidity	2	Vaisala ES 120 temperature and humidity sensor: range, -50 to +80 °C, 0 to 100%; precision, ±0.25 °C, ±0.3% ; response time, 5 s; mounted in a EA 130V radiation shield.
Air Temperature and Humidity	3	Vaisala HMP 113Y temperature and humidity sensor: range, -40 to +80 °C, 0 to 100%; precision, ±0.25 °C, ±0.2 to 0.3% ; response time, 5 s; mounted in a R. M. Young electrically aspirated radiation shield.
Humidity	4	Vaisala HMP 35A capacitance type sensor: range, 0 to 100%; response time, 5 s; precision, ±0.2 to 0.3% ; mounted in a EA 130V radiation shield.
Wind Speed and Direction	5	R. M. Young 05103 propeller and vane: range, 0 to 50 m s^{-1}; threshold sensitivity of propeller, 0.2 to 0.4 m s^{-1}, of vane, 0.7 m s^{-1}.
Wind Speed and Direction	6	Omnidata ES 050 propeller and vane: range, 0 to 40 m s^{-1}; threshold sensitivity of propeller, 0.4 m s^{-1}, of vane, 0.4 m s^{-1}.
Wind Speed	7	R. M. Young, Gill 3-cup anemometer: range, 0 to 50 m s^{-1}; threshold sensitivity, 0.5 m s^{-1}.
Wind Direction	7a	R. M. Young 12105, Gill microvane; range, 355 °azimuth, threshold sensitivity, 0.4 m s^{-1}.
Solar Radiation	8	Eppley Precision Spectral Pyranometer: range, with clear glass, 0.285 to 2.80 μm; temperature dependence, ±1% for -20 to +40 °C; linearity, ±0.5% from 0 to 2800 W m^{-2}; response time, 1 s.
Infrared Radiation	9	Eppley Precision Infrared Radiometer (Pyrgeometer): range, 4 to 50 μm; temperature dependence, ±1% for -20 to +40 °C; linearity, ±1% from 0 to 700 W m^{-2}; response time, 2 s.
Precipitation	10	Weathertronics Model 6028A heated tipping bucket gauge with 'Alter' type shield: 12 in. orifice; sensitivity, 0.25 mm/tip; precision, 0.5% at 0.5 in hr^{-1}.
Precipitation	11	Qualimetrics 6011b tipping bucket gauge with 'Alter' type shield: 8 in. orifice; sensitivity, 0.25 mm/tip; precision, 0.5% at 0.5 in hr^{-1}.

$$u^* = \frac{kU}{\ln((Z_m - d_0)/z_0) - \Psi_m((Z_m - d_0)/L)} \quad (1)$$

$$H = \frac{(T_a - T_s)\rho c_p k u^*}{\ln((Z_t - d_0)/z_{0t}) - \Psi_t((Z_t - d_0)/L)} \quad (2)$$

$$E = \frac{\rho k u^* (q_a - q_s)}{\ln((Z_v - d_0)/z_{0v}) - \Psi_v((Z_v - d_0)/L)} \quad (3)$$

where E is evaporation (kg m^{-2} s^{-1}); H is the sensible heat flux (W m^{-2}); T_a and T_s are the air and snow-surface temperatures (°K); U is wind speed (m s^{-1}); Z is the instrument height above the surface (m); c_p is the specific heat of air at constant pressure (1,005 J kg^{-1} ·°K^{-1}); g is the gravitational constant (9.806 m s^{-2}); k is von Karman's dimensionless constant (0.4); q_a and q_s are the specific humidity of the air and snow-surface; u^* is the friction velocity (m s^{-1}); z_0 is the applicable roughness length (m); ρ is the density of the air (kg m^{-3}); Ψ is the correction for atmospheric stability; and m, t and v are the respective subscripts for momentum, sensible heat and water vapor. Positive values signify a flux directed at the snow-surface. The value of L, the Obukhov stability length (m), is given by

$$L \equiv \frac{u^{*3}\rho}{gk((H/T_a c_p) + 0.61E)} \quad (4)$$

When surface irregularities are numerous and extensive, the base reference for measurement of Z lies between ground-level and the average height of the roughness elements, h_0; and the correction for this difference is called "displacement height" d_0. Brutsaert (1982) recommends $d_0 = 0.66\ h_0$ as an approximation, but for open snow-surfaces d_0 was much smaller than the measurement error in Z, and this correction was ignored.

When L is infinitely large the atmosphere is neutral and log-linear relationships for wind speed, temperature and vapor pressure extend throughout the lower surface sublayer. L is positive for stable conditions, and a decreasing magnitude indicates increasing stability; the closer the value to zero the more effectively turbulence is dampened and the greater the flux reduction. Negative L indicates instability, and its magnitude might be envisioned as the height at which buoyant forces first begin to dominate over those generated by shear (Brutsaert 1982). Shear forces are at a maximum near the surface, and a decreasing magnitude of L indicates increasing dominance by strong buoyant forces.

The Ψ corrections for a stable atmosphere were taken from Imberger and Patterson (1990)

$$\Psi = -5(Z/L); \qquad \text{for } Z/L < 0.5$$

$$\Psi = 0.5(Z/L)^{-2} - 4.25(Z/L)^{-1} - 7\ln(Z/L) - 0.825; \qquad \text{for } Z/L \text{ from } 0.5 \text{ to } 10$$

$$\Psi = \ln(Z/L) - 0.76(Z/L) - 12.093; \qquad \text{for } Z/L > 10 \quad (5)$$

These are the same equations given in Katul and Parlange (1992), corrected for continuity at the designated boundaries. Equal corrections were applied to all three fluxes, *i.e.* $\Psi_m = \Psi_t = \Psi_v$. Although some authors propose different functions for momentum and sensible heat or water vapor, we followed the recommendation of Brutsaert (1982): "that the differences between the functions in the stable case are less meaningful than those for instability, and until significant agreement and consensus develop, the assumption that the three are equal is conservative."

The corrections for an unstable atmosphere are from Brutsaert (1992). The Ψ function for specific heat and water vapor is different from the functions for momentum. For sensible heat and water vapor,

$$\Psi_t(Z/L) \quad \text{or,} \quad \Psi_v(Z/L) = 1.2 \ln\left(\frac{0.33+y^{0.78}}{0.33+y_0^{0.78}}\right) \tag{6}$$

For momentum,

$$\Psi_m(Z/L) = 0, \qquad \text{for } y < 0.0059 \tag{7}$$

$$\Psi_m(Z/L) \equiv 1.47 \ln\left(\frac{0.28+y^{0.75}}{0.28+(0.0059+y_0)^{0.75}}\right) - 1.29\left(y^{1/3} - (0.0059+y_0)^{1/3}\right) \tag{8}$$

$$\text{for } 0.0059 \leq y \leq 15.025$$

$$\Psi_m(Z/L) = \Psi_m(15.025), \qquad \text{for } y > 15.025 \tag{9}$$

where $y = -Z/L$, $y_0 = -z_0/L$ and z_0 is the respective roughness length for either sensible heat and water vapor or momentum.

Eqs. (1)-(4) are solved by iteration. The Ψ functions are initially set to zero, *i.e.* a neutral atmosphere is assumed, and the fluxes calculated with Eqs. (1)-(3). The Obukhov length is computed using these values in Eq. (4), and the Ψ corrections for the next iteration are calculated. When the difference between successive values of L reaches an acceptable limit, the iteration can stop. For certain combinations of weather parameters (stable conditions and light winds), the iterative procedure may fail to close, and a maximum value for the Ψcorrection, or a limit on the number of iterations, can be imposed.

Roughness Length

The momentum roughness length, z_0, of snow varies from 0.0001 to 0.02 m (Moore 1983; Morris 1989). Generally, lengths around 0.001 m are used for "smooth" snow, ~0.005 m for surfaces described as undulating, suncupped or hummocked; terrain obstacles or protruding vegetation further increase the value. With one exception, a roughness length of 0.005 m was used throughout the analysis.

The exception was at Wolverton where surrounding trees dictate a wind profile characterized by high z_0 and significant vertical displacement of the reference level

from the ground, d_0. Roughness lengths for forested areas are typically within a range of 0.4 to 1.2 m (Brutsaert 1982; Parlange and Brutsaert 1989). At Wolverton, z_0 was set at 0.5 m and the displacement height calculated as $d_o = 4.9z_0$ (Brutsaert 1982).

Theoretical considerations indicate that roughness lengths for sensible heat and vapor should be one to two orders of magnitude smaller than for momentum (Moore 1983; Brutsaert 1982). As an empirical example, Pluss and Mazzoni (1994) calculated z_0 values of $\sim 10^{-3}$ m compared with z_{0t} values $\sim 10^{-6}$ m. In this study, the roughness lengths for sensible heat and water vapor were assumed to be a tenth of that for momentum ($0.1z_0$).

Snow Surface Temperature

Because the meteorological data were collected at a single-level above the surface, the second reference point for the solution of Eqs. (2) and (3) is the surface itself, or more precisely, a distance equal to the roughness length above the surface. In the absence of snow-surface temperature measurements, a simple model (*s*Temp 1) accounting for the observations that night-time snow-surface temperatures are 4 to 6°C below the air temperature (Bernier and Edwards 1990) and snow-surface temperatures lag changes in air temperature (Marks and Dozier 1992), was used:

1800-1945 hrs: 2 degrees below the air temperature
2000-0400 hrs: 4 degrees below the air temperature
0545-0600 hrs: 2 degrees below the air temperature
at all other times:

$$T_{snow} \equiv T_{snow(n-1)} + 0.5(T_{air(n)} - T_{snow(n-1)}) \qquad (10)$$

$$\text{if } T_{snow} > 0^{\circ}C, \quad \text{set } T_{snow} = 0^{\circ}C$$

Modeled snow-surface temperatures were compared with measurements from CSSL (Fig. 2). As snowmelt progresses, snow-surface temperatures are constrained at zero an increasing percentage of the time, and the mean-profile results are less dependent on the surface temperature model.

Specific Humidity

Specific humidity can be expressed as (Saucer 1955)

$$q = \frac{0.622 f_w e}{p - 0.378 f_w e} \qquad (11)$$

where f_w is a correction factor applied to the universal gas constant, and e and p are the vapor and barometric pressures (mb). Since f_w is near unity, and e is small compared with p, the equation can be simplified as

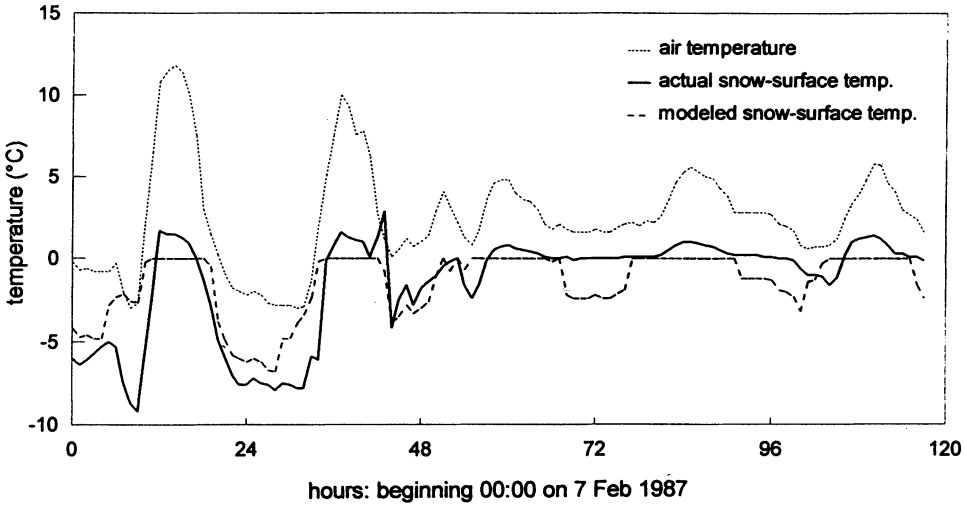

Fig. 2. Surface air temperature and observed and modeled snow-surface temperatures for 5 days in February 1987 at Tahoe, CA (data from the CSSL).

$$q = \frac{0.622e}{p} \tag{12}$$

Barometric pressure was not recorded at any of the weather stations; instead, average sea-level pressure, corrected for altitude at each site, was used as a constant (Morton 1983). Atmospheric vapor pressure was calculated from the air temperature and relative humidity. Similarly, snow-surface vapor pressure was assumed to be the saturation vapor pressure for ice at the snow surface temperature. Saturation vapor pressure was calculated as (Saucer 1955)

$$e_{sat} = 6.11 \times 10^{(aT/(T+b))} \tag{13}$$

where temperature is in °C, and a and b are constants: for water vapor over water, a = 7.5 and b = 237.3; over ice, a = 9.5 and b = 365.5.

The Density of Air

Since an average barometric air pressure was used, the equation for air density (Saucer 1955) was simplified to

$$\rho = 0.3484 \left(\frac{p}{T_a} \right) \tag{14}$$

where ρ is the density of moist air (kg m^{-3}), and T_a the air temperature (°K).

Results and Discussion

The mean-profile evaporation estimates for Emerald and Spuller lakes, SNARL, and Mammoth Mountain are shown as period evaporation (Figs. 3a-d). Each month was divided into 3 periods, *i.e.* the first 10 days, the second 10, and the remaining days, and period evaporation (in mm of water equivalent) is the sum of hourly calculated evaporation over each period (except at Mammoth Mountain where 15-minute data were summed). Gaps indicate missing meteorological data; proximity of maintenance personnel and climate severity were the key determinants of record completeness.

The general pattern was of higher evaporation during mid-winter, when vapor pressure differences were greatest, followed by continuously declining evaporation throughout snowmelt. Near the end of snowmelt, condensation of water vapor onto the snow-surface often matched evaporative loss and sometimes exceeded it. With the exposure of significant amounts of bare ground, atmospheric vapor pressures appreciably increased: a combined effect of high evaporation from moist snow-free areas, and increased air temperatures due to seasonal trends and sensible heat exchange. Higher atmospheric moisture content decreased the vapor pressure gradient over the remaining snow. Evaporation rates throughout April and into May were highest in 1993, when an above average snowpack maintained nearly complete snow coverage.

Condensation was prevalent at Mammoth Mountain in the late spring and summer. Although the persistence of snow into summer increases the probability of condensation, the primary cause was high humidity carried by prevailing westerlies. These winds are funneled through a low altitude pass, and by May are sufficiently warm to carry significant moisture. For example, vapor pressures in March and April of 1993 were normally distributed with median values ~3.7 mb; in May, the median vapor pressure increased by 50% to 5.58 mb, with a distribution skewed towards higher pressures. In contrast, median vapor pressure at Spuller in May was ~3 mb. Winds at Spuller are mostly down-canyon northwesterlies, relatively depleted in moisture after passing over the Sierra Nevada crest (~3,800 m).

With the exception of April in both 1991 and 1993, monthly evaporation at SNARL (Fig. 4a) varied between 5 and 20 mm. Higher April evaporation in 1991 was caused by two days of "chinook" conditions: dry, high-speed winds. Average evaporation over the two days was approximately 4 mm day^{-1}. In April 1993, two separate chinook events, averaging 3 mm day^{-1}, similarly increased evaporation.

Wind speed and atmospheric vapor pressure differences accounted for the variation in monthly evaporation between weather stations in 1993 (Figs. 4b and 5b). Wolverton, with the lowest mean wind speed and highest mean vapor pressure, had the lowest evaporation. Trees surrounding this site dampen turbulence and maintain high humidity above the snow surface. At Emerald, higher wind speed and lower vapor pressure increased evaporation, but the total remained low, *i.e.* 62 mm, Novem-

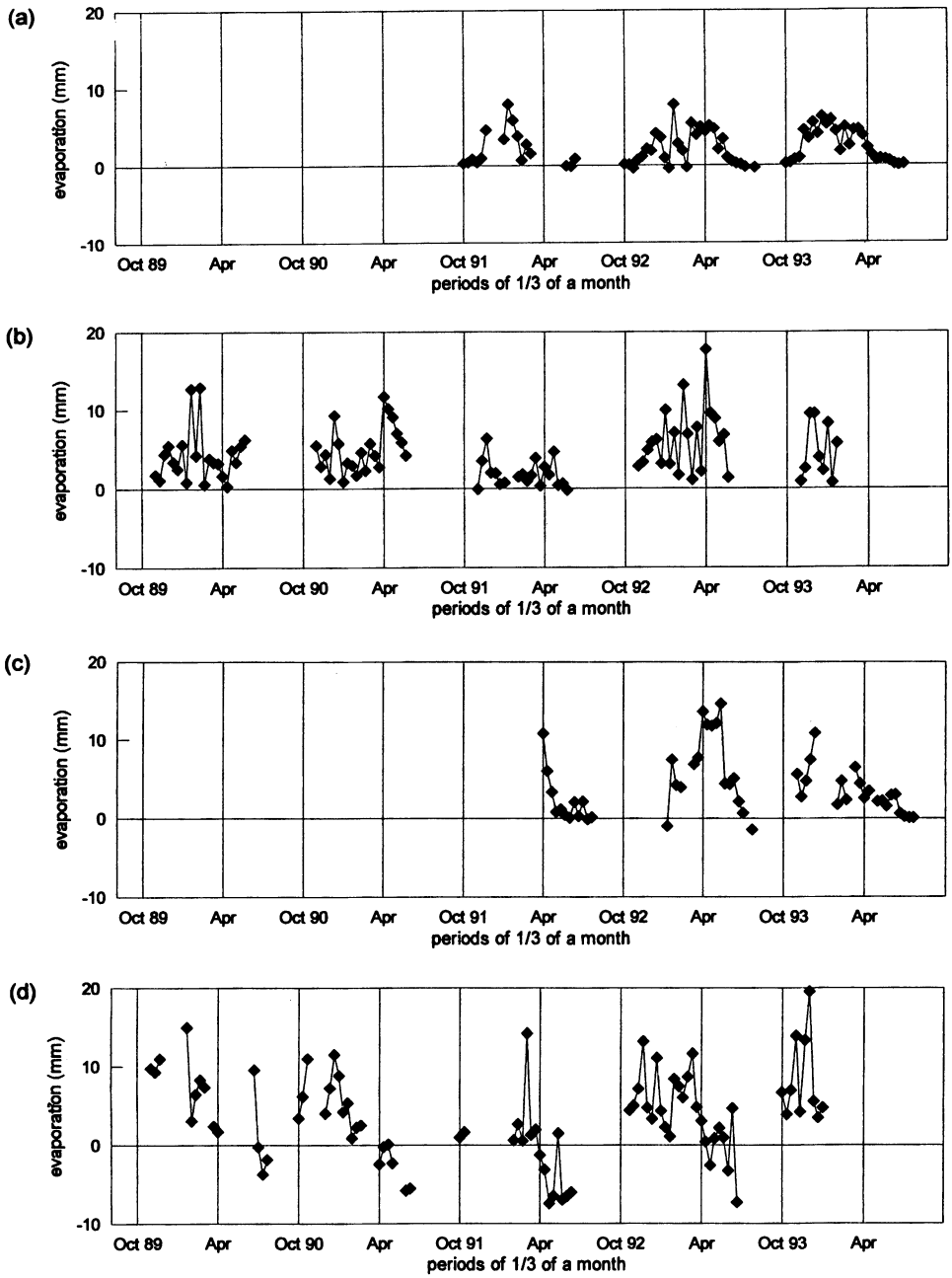

Fig. 3. Snowpack evaporation in mm of water equivalent lost over each ~10-day period at a) Emerald Lake, b) SNARL, c) Spuller Lake and d) Mammoth Mountain. Points represent the sum, for each period, of hourly (15 minutes at Mammoth) mean profile estimates. Negative values indicate condensation.

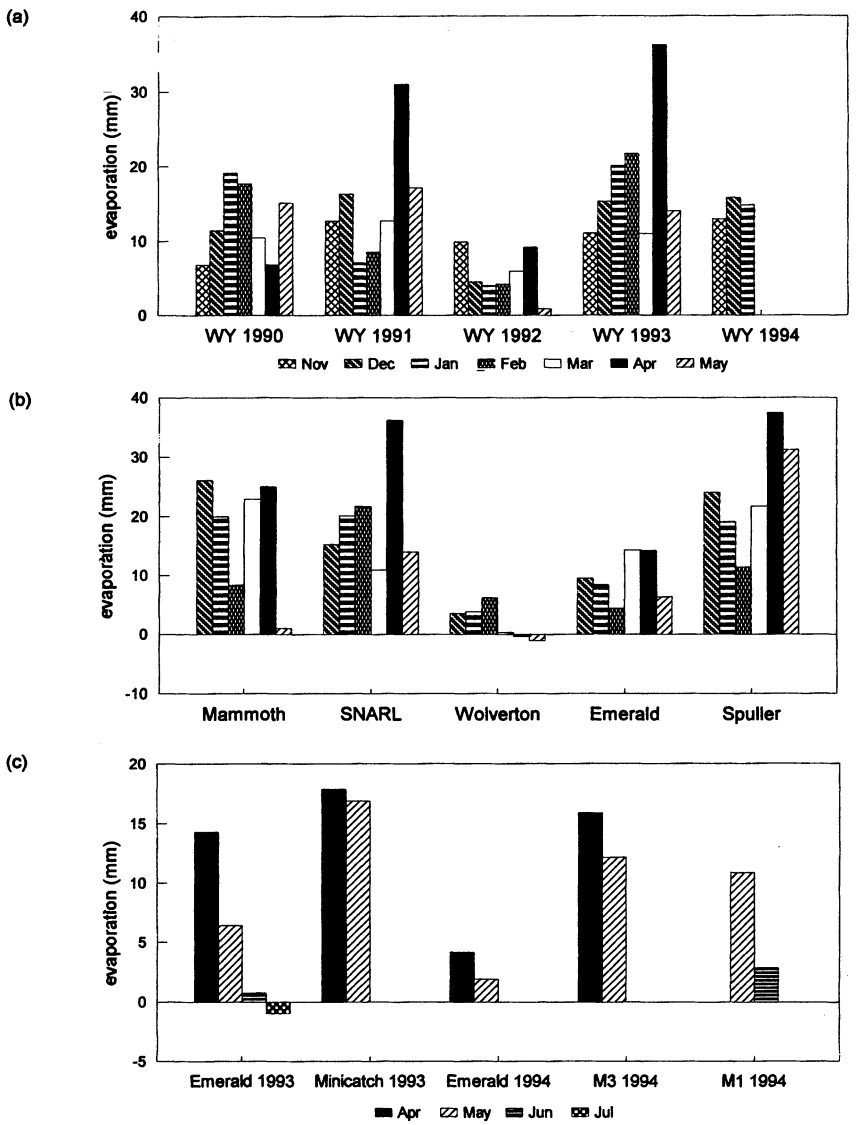

Fig. 4. a) Monthly snowpack evaporation, in mm of water equivalent, for 4+ seasons at SNARL (snow was assumed to be present during some snow free intervals). b) Monthly snowpack evaporation during water year 1993 at 5 southern Sierra Nevada sites; snow was present at the higher elevation sites past May, but to simplify the comparison these results are not shown. c) Comparison of monthly snowpack evaporation during snowmelt at Emerald with other locations in the same basin (evaporation was equal to condensation at Emerald in June 1994). All monthly totals are summations of hourly mean profile estimates (15 minutes at Mammoth and the mini-catchments). Negative values indicate condensation.

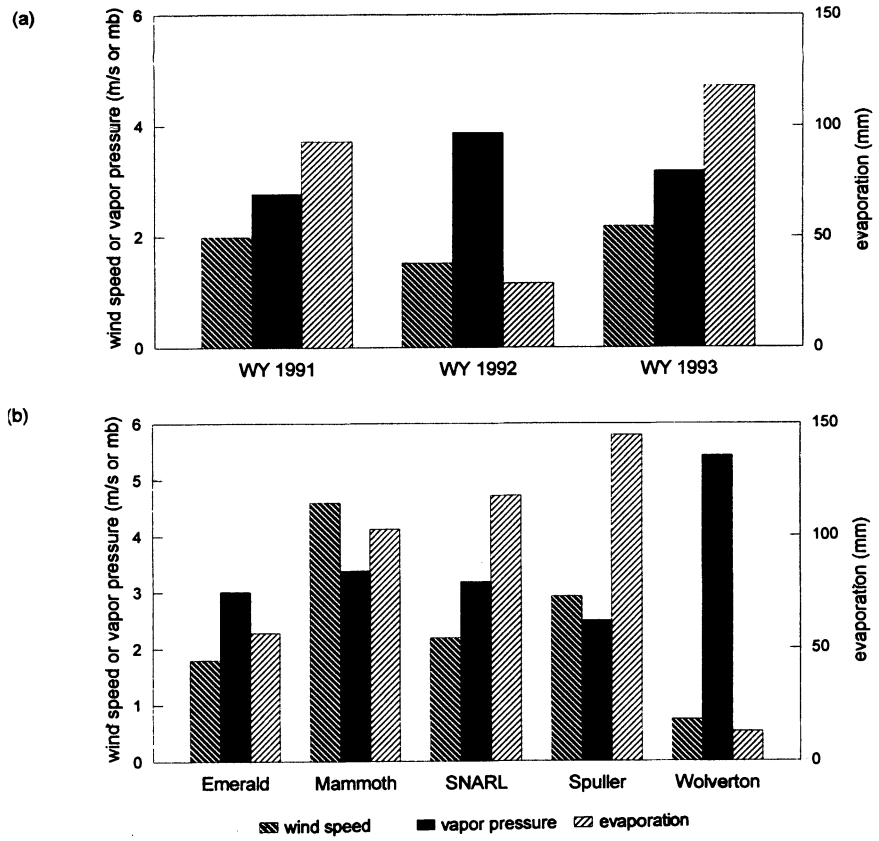

Fig. 5. a) Mean wind speed, mean vapor pressure and total estimated evaporation (Dec. through May) for three water years at SNARL. b) Mean wind speed, mean vapor pressure and total estimated evaporation (Dec. through May) at five southern Sierra Nevada sites during water year 1993.

ber through July. The other weather stations, exposed to higher winds, had losses two to three times higher: total evaporation at Mammoth, SNARL and Spuller was 112, 129, and 156 mm, respectively. Although wind speed at SNARL was less than half that at Mammoth, evaporation was higher due to the April chinook intervals and lower mean vapor pressure. The highest evaporation occurred at Spuller, consistent with the driest air and the second highest wind speeds. Annual differences also reflected changes in mean wind speed and vapor pressure, *e.g.* at SNARL (Fig. 5a).

Station mean wind speed in 1993 (December through May) varied from 0.74 to 4.6 m s^{-1}. Except for Wolverton, the frequency distributions of hourly wind speed (15 minutes at Mammoth) are similar (Fig. 6a). Frequency distributions of temperature were also similar (Fig. 6c); the Wolverton distribution is slightly skewed towards higher temperatures due to lower elevation while the increased kurtosis at

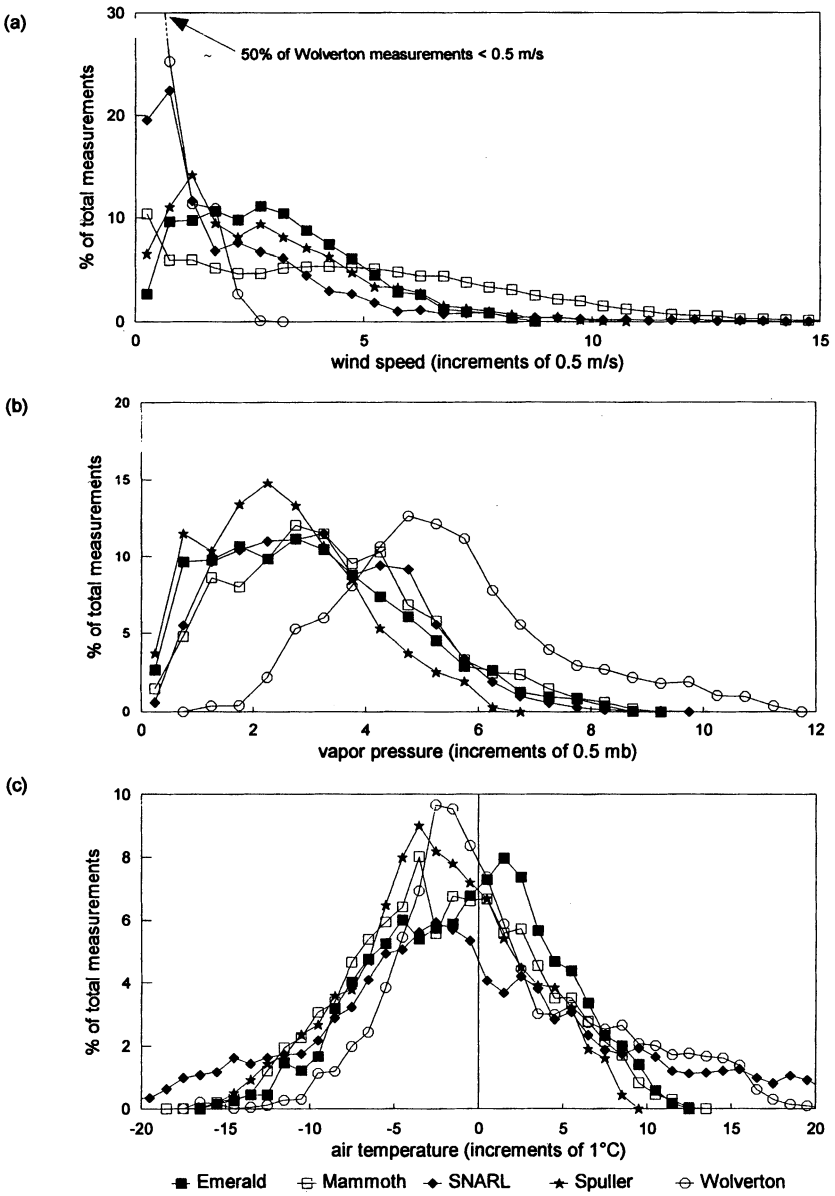

Fig. 6. Distributions of hourly (15 minutes at Mammoth) mean a) wind speed, b) vapor pressure and c) air temperature for five southern Sierra Nevada weather stations during December through May of water year 1993.

SNARL is caused by lower elevation and nocturnal valley cooling. Only at Wolverton and Spuller were the vapor pressure distributions noticeably different, with higher and lower values, respectively (Fig. 6b).

Table 4 – Annual water year evaporation from snow (mm of water equivalent) at the study sites. The total for the accumulation season (winter) is followed by the total evaporation during snowmelt. The maximum snowpack accumulation at each location (m of snow water equivalent) is given in parenthesis. Negative values indicate condensation, missing values indicate incomplete or missing data.

	1990	1991	1992	1993	1994
Emerald Lake			53, 13 (0.7)	41, 21 (1.4)	52, 14 (0.8)
SNARL	48, 8 (0.2)	30, 12 (0.3)	20, 7 (0.2)	66, 29 (0.8)	45, -- (0.4)
Spuller Lake			--, 27 (0.6)	102, 54 (1.7)	88, 21 (0.7)
Mammoth	112, -8 (0.8)	81, -19 (1.0)	89, -27 (0.8)	122, -10 (2.4)	104, -16 (1.1)

In 1993, meteorological data were collected at a ridge-top location 2 km north of Emerald Lake (identified as the mini-catchments) and in 1994, at two sites, 2.5 and 4 km from Emerald, on a high plateau to the east (respectively, M1 and M3). Although these locations had higher wind speeds and lower vapor pressures than Emerald, monthly evaporation was also low (Fig. 4c). The greatest differences (May 1993 and May and June 1994) resulted from higher Emerald vapor pressures rather than lower wind speeds.

Excluding Wolverton, annual evaporation from snow fell within a range of 27 (SNARL 1992) to 156 mm (Spuller 1993). The lower estimate is from a shallow, low-elevation snowpack, the upper from a high-elevation location characterized by high winds and low vapor pressures. Our estimate of a regional mean would lie between evaporation at Emerald and evaporation at Spuller (Table 4): 80 to 100 mm of annual loss.

During the drought years of 1990 through 1992, maximum snow accumulation varied from 0.6 to 1.0 m (water equivalent). Our lower estimate of regional evaporation (80 mm, assuming a shortened snow-cover season) gives a snowpack loss of 8 to 13%. In the high snowfall year of 1993, peak accumulation varied from 1.4 to 2.4 m, and an evaporation estimate of 100 mm amounts to an average loss of 4 to 7%. During snowmelt, average evaporation at Emerald and Spuller was 16 and 34 mm, respectively. An estimated average regional loss of 25 mm represents 3 to 4% of the snowpack during drought years, 1% for above normal accumulations. None of these estimates include losses that occur during the re-deposition of wind blown snow (heavy snow density and the relative absence of major wind scour and depositional patterns in these catchments lead us to believe that these losses were minor).

Sensitivity of Evaporation to Model Assumptions

The sensitivity of calculated evaporation to the estimated model parameters was evaluated with two data sets: Emerald from January through April of 1993, and Wolverton during January, March and April of 1993. A constant instrument height was assumed except when sensitivity to instrument height was specifically examined.

Roughness Length

Evaporation at Emerald was calculated for momentum roughness lengths from 0.0001 to 0.9 m (Fig. 7a). At high values (> 0.1 m), increases in z_0 cause large increases in total evaporation, as the velocity and humidity profiles abruptly steepen. However, within the range of probable roughness lengths, 0.001 to 0.02 m, changes are small: evaporation doubling over this span.

At Wolverton, probable values of z_0 vary from 0.1 to 1.0 m, and evaporation increases by 500% over this interval (Fig. 7b). The effect of increasing z_0 is magnified by increases in displacement height, set at 4.9 z_0. Since a fixed anemometer height was assumed (7.7 m), higher values of z_0 dramatically steepen the wind profile and increase calculated evaporation. Although the model is sensitive to the chosen value of z_0 at Wolverton, evaporation is so low as to make little overall difference. A doubling of z_0 would have increased evaporation from 4 to 7 mm.

We also assumed a ratio of 0.1 for z_{0t}/z_0 and z_{0v}/z_0. For the roughness length used in analyzing all but the Wolverton data (0.005 m), varying the ratio by an order of magnitude changed evaporation by ~12% (Fig. 7c). For larger z_0 the change in evaporation becomes progressively greater: a 50 per cent increase for a z_0 of 0.1 m (Fig. 7d). However, such large z_{0v} values are improbable. The Wolverton results were similar.

Wind Speed

Wind speed is the critical variable; all of the fluxes are directly proportional to wind speed and the Obukhov length is proportional to its third power. Wind reduces the importance of atmospheric stability; with increasing wind speed, turbulent shear forces become dominant and the atmosphere approaches neutrality. A graph of evaporation *vs.* average wind speed for Emerald was developed by multiplying the hourly wind speeds by a variable "wind speed factor" (from 0.1 to 10) and recalculating evaporation (Fig. 7e). Doubling the wind speed tripled the evaporation. The reliability of the evaporation results, therefore, rest heavily on anemometer accuracy.

Inaccurate, misplaced or improperly installed anemometers could lead to erroneous conclusions. We used 12 anemometers of 4 types, at times using 2 or 3 at an individual site. We regard our findings of low average wind speeds in this region as well founded. Average evaporation of 2 mm day^{-1} at Emerald (Kattleman and Elder 1991) would have required a mean wind speed of 7.5 m s^{-1} over the four month data set (Fig. 7e) if other factors remained unchanged. Speeds this high occur, but rarely and in isolated locations, *e.g.* wind speed at Mammoth Mountain during the 1993 snow season exceeded 7.5 m s^{-1} only 20% of the time.

Instrument Height

Daily measurements of snow depth were made at Lodgepole Ranger Station, close to Wolverton. This record helped determine the relative snowpack fluctuation between major storms. When combined with measurements made during site-visits, it

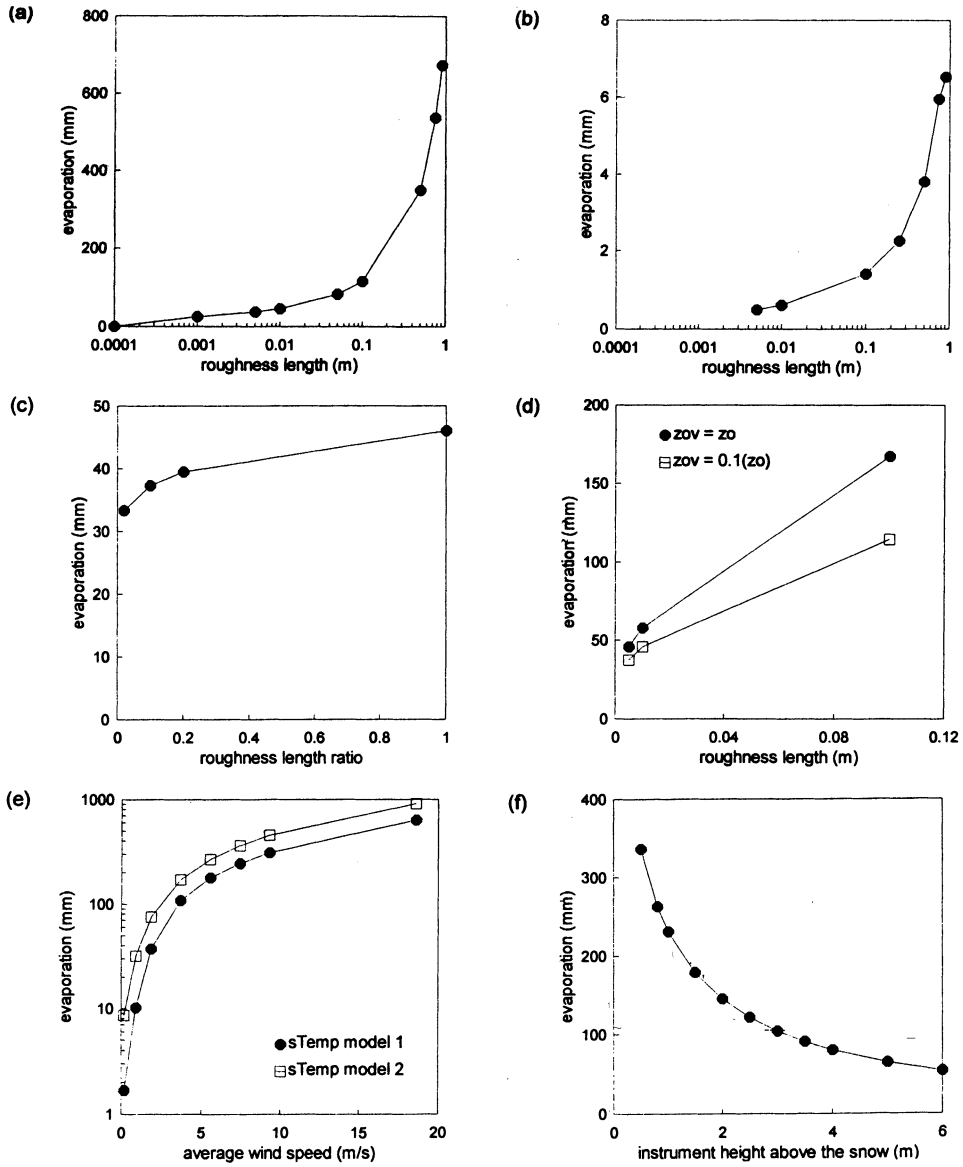

Fig. 7. The sensitivity of the mean-profile estimates of evaporation to a) momentum roughness length at Emerald, b) momentum roughness length at Wolverton, c) the ratio of the vapor roughness length, z_{0v}, to that for momentum, z_0, at Emerald; d) momentum roughness length for different roughness length ratios, (z_{0v}/z_0) at Emerald; e) wind speed at Emerald; and f) instrument height at Emerald. The ordinates represent total snowpack evaporation from January through April at Emerald, or from January, March and April at Wolverton.

was used to reconstruct snow depth at each of the weather stations. Since instrument height errors did occur, Emerald data were used to evaluate their effect on calculated evaporation (Fig. 7f). If instrument height is underestimated, the wind speed, temperature, and vapor profiles steepen, increasing the calculated fluxes. However, only when the instruments are close to the snow-surface will small errors in height produce large changes in evaporation. At Emerald, the meteorological instruments were 5 to 6 m above-ground and the maximum snow-depth varied from 1.5 to 3 m.; for this range, an instrument height error of ±1 m changed evaporation by approximately 20%.

Snow Temperature

Emerald evaporation calculated with the snow-surface temperature model of Marks *et al.* (1992; *s*Temp 2) was double the evaporation calculated using *s*Temp 1 (Eq. (10)). Marks *et al.* assumed that turbulent exchange takes place, not at the snow-surface, but 15 to 25 cm below the surface, *i.e.* within a porous upper layer. Their model was based on measurements within this layer. The difference between models is not about snow-surface temperature, *per se*, but air temperature at the snow-surface, and what snowpack strata corresponds with, and determines it.

Differences in calculated evaporation using the two models vary with wind speed and season. At low wind speeds the difference was substantial, on the order of a few hundred per cent, but declined to a constant 50% at wind speeds greater than 5 m s^{-1} (Fig. 7e). With *s*Temp 2, snow temperature always lags air temperature, producing snow temperatures above the air temperature for a majority of the hourly accumulation season intervals. This has two effects: it produces neutral or unstable conditions much of the time, and it greatly enhances vapor pressure differences during these periods.

During the 1993 snow accumulation season, *s*Temp 1 produced stable conditions 82% of the time, compared with 47% for *s*Temp 2. Halving the occurrence of atmospheric stability accentuates evaporation at low wind speeds when the role of instability is enhanced. For Wolverton, which exemplifies this situation, *s*Temp 2 increased evaporation six fold over that calculated with *s*Temp 1: from 4 to 22 mm. The instability effect and the large thermal lag used in the Marks *et al.* model maximized evaporation and set an upper limit on the probable snow-surface temperature error. Varying the parameters of *s*Temp 1 and *s*Temp 2 resulted in evaporation estimates between the bounds set by the original models. Maximum evaporation, obtained by setting accumulation season snow-surface temperature to a constant 0°C, was twice the *s*Temp 2 estimate. During snowmelt, both models are increasingly constrained to 0°C and there was little difference in calculated evaporation.

Different snow temperature assumptions are responsible for only a small part of the large difference in calculated evaporation between the two studies at Emerald. Marks *et al.* (1992) report a total evaporation from November 1985 through April 1986 of 300 mm of water. In 1993, a similar snow year, our study showed a total of

55 mm for the same period. Using *s*Temp 2 increased the total to 110 mm. During the remainder of the snow season (May through July), when both temperature models would have estimated similar snow-surface temperatures, the differences between the studies were larger: 155 mm *vs.* 6 mm.

The principal disagreement lies in the measurement of wind speed. Marks *et al.* measured wind at two sites, described as "ridge" and "lake" locations. The respective means (and range), for hourly wind speed from December through May 1986, were 7.5 m s^{-1} (2.0 to 16.9 m s^{-1}), and 5.0 m s^{-1} (1.3 to 9.4 m s^{-1}). In contrast, mean hourly wind speed measured in this study, for the same months in 1993, was 1.8 m s^{-1} (0 to 13.8 m s^{-1}). Wind speed differences account for the different evaporation results. Their average wind speeds seem anomalously high, based on the multiple sites and years of our study.

Mean-Profile Assumptions and the Mountain Environment

The assumptions of steady-state flow and homogeneous surface conditions used to develop the mean-profile equations are violated in a mountain environment. The steady-state requirement is impossible to satisfy, but most authorities feel that ignoring it introduces little error (Moore 1983); Brutsaert (1982) recommends using averaging times of 20 to 60 minutes as a good compromise between reasonably constant atmospheric conditions and adequate sampling. The time interval used for averaging meteorological data in this study followed his recommendation: 60 minutes, except at Mammoth and the mini-catchments where a 15-minute interval was used. A test using 15 *vs.* 60 minute Mammoth data showed little difference in calculated evaporation. The second assumption is more critical. While snow reduces small scale differences by smoothing terrain features and covering vegetation, mountain surfaces are not homogeneous.

A change in surface forces the development of a "transition zone" (Oke 1987), where the overpassing air reflects a mixture of both old and new surface characteristics. Below this zone the air is fully adjusted to the new conditions, above it, it reflects only the conditions of the old. The top of the transition zone develops at a rate of 1 m vertically for every 10 to 30 m of horizontal travel past the boundary, but the fully adjusted layer grows more slowly, 1 m vertically for every 100 to 300 m (Oke 1987); although with rougher surfaces and unstable conditions, vertical development may be more rapid. To ensure fully adjusted conditions for instruments ~3 m above the snow surface, at least a few hundred metres are needed for an adequate fetch. Many of the measurements in our study did not meet this criteria.

Meteorological instruments in a transition zone record a spectrum of prior changes in surface and slope, and the principal mean-profile errors will lie in the assumptions of instrument height and surface roughness. We estimate the effect of the combined error on calculated evaporation as less than 20% (Figs. 7a and 7f). That the measured meteorological variables represent values integrated over a range of terrain may even be an advantage, since the overall objective of the study is not the ac-

curate calculation of point evaporation, but a broader based estimate.

Radiative Heating above the Snow Surface

Halberstam and Schieldge (1981) performed extensive profile measurements over a melting snow surface in an open field near Lee Vining, California, in March 1978. They reported anomalous temperature profiles, with a persistent warm layer forming ~0.5 m above the snowpack on clear, calm days. Their interpretation was that under conditions of initial stability, evaporated water vapor was retained in the air layer just above the snow-surface and subsequently heated by solar radiation, directly from above and by reflection off of snow. As the layer became warmer than either the snow surface or the ambient air above, it re-radiated energy in the infrared from its upper surface towards the atmosphere and from its lower, towards the snowpack. Others have reported the same phenomenon (Male and Granger 1979).

These conditions would introduce error into a single-level calculation of the sensible heat flux. Typically during snowmelt, the single-level model portrays stable conditions and a near-logarithmic temperature profile. With a radiatively heated layer, a sensible heat flux reversal occurs at the temperature maximum: stable air and a strong flux towards the surface below the layer, and unstable conditions and an upward flux above it. Thus a single-level model underestimates the sensible heat flux. Male and Granger (1978) suggest using a second temperature sensor at a distance of 10 to 30 cm above the snow to overcome this difficulty.

The effect of this problem on the water vapor flux is less clear. Increased turbulence above the temperature maximum enhances evaporative transport, yet moisture retention in the lowest air layer is necessary to maintain the maximum. Stable conditions below the temperature maximum and the maintenance of a high vapor pressure in this layer would indicate little additional vapor flux from the surface itself. Moore (1983) states that under the initial conditions necessary for the formation of this maximum, the turbulent fluxes are of minor importance to the overall energy balance and that, when they become important, on windy overcast days, this condition cannot develop.

At Emerald, during the later part of May and into June 1994, three temperature sensors were installed, the lower sensor ~0.5 m above the surface. During this period, late afternoon wind speeds were low (typically <0.5 m s^{-1}), ideal for developing a radiation maximum. Night-time temperatures at the lowest sensor level were usually lower than temperatures recorded at the sensor above, as expected under stable atmospheric conditions. However, beginning just before noon, the reverse often occurred: the lower sensor recording warmer temperatures (Fig. 8). Days when this pattern did not develop or developed differently were characterized by either much higher wind velocities or consistently low wind speeds throughout the day. The radiation maximum was neither as well developed nor as persistent as at Lee Vining (~1 *vs.* 3 to 4°C).

Weather instruments were intermittently maintained at multiple levels during

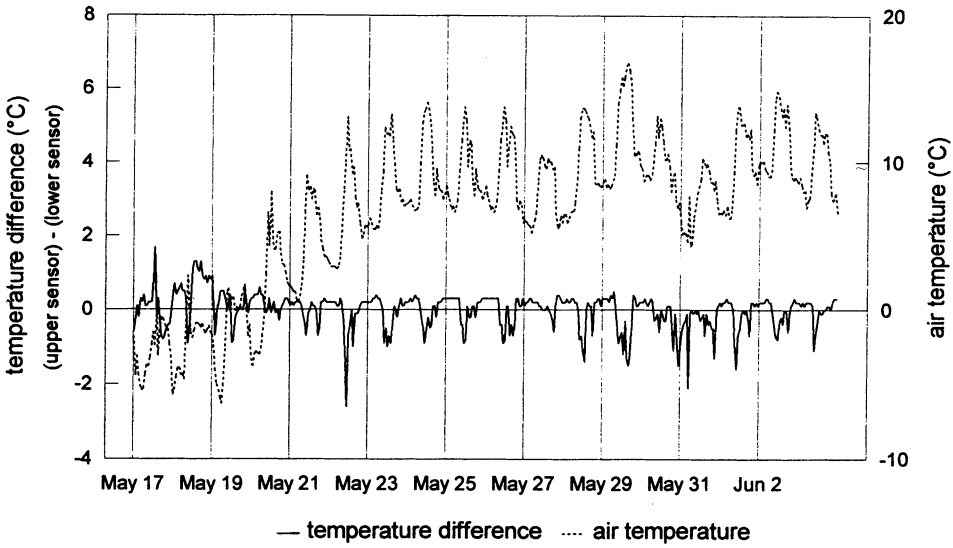

Fig. 8. The difference in mean hourly air temperature between the upper and lower sensors at the Emerald meteorological station from May 17 to June 3, 1994. The vertical grid lines mark 00:00 hrs. The lower sensor was 0.67 m above the snow at the beginning of the period, 1.07 above at the end; the upper sensor was 1.55 m above the lower. Negative temperature differences indicate a higher temperature at the lower height and the presence of a radiative heated layer above the snow.

snowmelt at Emerald in 1993 and at the mini-catchments in 1994; for these intervals, we separately calculated total evaporation and sensible heat transfer for each level (Table 5). The Emerald data show differences in the specific heat flux for different sensor heights, as predicted for a radiation maximum. However, the evaporation differences are small enough to have been caused by instrument variation and other errors. At the mini-catchments, a greater sensible heat flux was calculated for the higher sensor, the opposite of what was expected with a radiation maximum. Higher wind velocities at the site may be preventing its development. The small differences in calculated evaporation for different sensor levels argue for the relative insensitivity of our results to the radiation maximum problem.

Model Accuracy

The mean-profile evaporation estimates of our study cannot be independently verified. Combination methods such as Penman's add a radiation balance to the turbulent flux calculations, increasing both the probability of error and the reliance on estimated snow-surface temperature. Other authors report poor success with the Bowen ratio (Male and Granger 1979; McKay and Thurtell 1978). Calculating evaporation is problematic for Bowen ratios of -0.5 to -1.0, the expected range during snow accumulation when the water vapor and sensible heat fluxes are nearly identi-

Table 5 – Total evaporation and sensible heat fluxes for the given periods and locations. The fluxes were calculated for different sensor heights with the single-level mean-profile equations. Positive values signify a flux directed towards the snow surface.

site	period	sensor ht. (m)	evaporation (mm)	sensible heat (MJ m^{-2})
Emerald Lake	May 1994	4.15	-0.86	+2.16
	(16 days)	2.22	-1.77	+6.35
		0.67	-4.14	+17.21
Emerald Lake	June 1994	4.90	+0.06	+3.05
	(16 days)	2.62	-0.01	+6.18
		1.07	-0.47	+13.27
Mini-catchments	April 1993	2.50	-17.92	+30.85
	(23 days)	1.20	-12.26	+18.83
Mini-catchments	June 1993	4.34	-0.35	+3.52
	(4 days)	1.85	-0.10	+1.53

cal but opposite in sign (Cline 1995; Marks and Dozier 1992). Net radiation is also required, dependent, as is the Bowen ratio, on estimated snow-surface temperatures. Eddy flux correlation can directly measure evaporation from the instantaneous fluctuations of both vertical air speed and water vapor density. However, the instrumentation is difficult to maintain and a large power requirement makes it unsuitable for remote locations.

Few evaluations of mean-profile results using sensors at a single-level are available. Pluss and Mazzoni (1994) compared single-level flux calculations during snowmelt with those obtained using sensors at four levels and found a "systematic overestimation." They felt that the results for sensible heat were better than for vapor. Comparisons between eddy correlation and the 4-level profile were generally good: somewhat overestimating larger and underestimating smaller fluxes. Some researchers have used lysimeters to verify the energy balance during snowmelt. However, single lysimeters are undependable and small amounts of evaporation cannot be distinguished within the standard error of even extensive arrays (Kattelmann 1995).

Snowmelt models, such as SNTHERM (Jordan 1991), calculate evaporation with single-level meteorological data using the energy balance to derive snow-surface temperature. Cline (1997) found that SNTHERM snowmelt evaporation closely matched his multi-level mean-profile calculations. However, besides meteorological data and long- and short-wave radiation, the model requires snow-profile data for initiation (layer-by-layer input of temperature, crystal size, and density). In our study, snow-profile data were only available (except at Mammoth) for the snowmelt season, when the snow-surface temperature is easily modeled.

Using values from the sensitivity analysis of evaporation to the model assumptions, and adding a similar analysis for instrument errors, we estimate that the com-

Table 6 – Estimated errors in calculated evaporation (± %) attributed to instrument errors and the mean-profile assumptions. The combined error was calculated using the root-sum-square method. The percentage error is given for both reasonable and high estimates of the individual errors.

	accumulation season (winter)		snowmelt season	
item	reasonable	high	reasonable	high
specific humidity	5	5	5	5
wind speed	30	30	30	30
snow-surface temperature	25	60	5	10
instrument height	10	20	5	10
roughness length (z_0)	10	25	10	25
roughness length ratio (z_{0v}/z_0)	6	6	6	6
combined probable error	42	75	33	42

bined probable error in winter (accumulation season) evaporation lies between 40 to 75%, while that for the snowmelt season is between 30 and 45% (Table 6); the lower value in the range is based on our estimate of the most reasonable magnitude of the individual errors while the upper represents the highest errors likely to have occurred. Given the low evaporation estimates for the study sites, even larger errors would not change the overall conclusions.

Conclusion

Only a small percentage of the settled snowpack was lost to evaporation. The average regional evaporative loss is estimated at 80 to 100 mm of water equivalent, ~7% of the maximum accumulation during an average snow year. During drought years the loss was less, but represented a greater percentage of the maximum accumulation, 8 to 13%. For years with above average snowfall, the loss decreased to about 4%, although the extended length of the snow season increased the actual amounts lost. Most of the evaporation occurred during the period of snow accumulation when vapor pressure gradients were usually favorable and conditions of atmospheric instability often occurred. Even so, small vapor pressure differences and relatively low wind speeds limited evaporation.

During snowmelt, increasing atmospheric stability and the reduction of the vapor pressure gradient due to the higher vapor content of the warming spring air reduced evaporation from snow to negligible amounts. Often near the end of snowmelt, snowpack losses from evaporation were exceeded by gains from condensation. Total losses from the snowpack during the snowmelt season were typically around 25 mm of water, representing 3 to 4% of the maximum accumulation during drought years, ~1% for above normal accumulations.

Acknowledgments

Funding for this work was provided by the National Aeronautics and Space Administration (NAGW-2602) and the California Air Resources Board (A032-188). Dan Dawson and Rick Kattelmann supplied much of the eastern Sierra data, and Jim Sickman, John Stoddard and Aaron Brown, along with their able field personnel, supplied data for the western slope. We thank Jim Sickman for his help and companionship throughout the years of the project and C. B. Beaty from whom we "borrowed" the idea of contrasting the quotes from Matthes and Sharp. We also thank J. Dozier, R. Bales, E. Andreas, B. Davis, R. Jordan, R. Kattelmann and M. Williams, along with two anonymous reviewers, who reviewed earlier drafts of this paper. The cooperation of Sequoia National Park and the Inyo National Forest was vital to the study and is gratefully appreciated.

References

Anderson, E. A. (1976) A point energy and mass balance model of a snow cover, Technical Report NWS 19, National Oceanic and Atmospheric Administration, Washington, DC.

Bernier, P. Y., and Edwards, G. C. (1990) Differences between air and snow surface temperatures during snow evaporation, *Can. J. Forestry Res., Vol. 20*, pp. 117-120.

Brutsaert, W. (1982) *Evaporation into the Atmosphere*; D. Reidel, Hingman Mass.

Brutsaert, W. (1992) Stability correction functions for the mean wind-speed and temperature in the unstable surface layer, *Geophys. Res. Lett., Vol. 19*, pp. 469-472.

Cline, D. (1995) Snow surface energy exchanges and snowmelt at a continental alpine site, In: *Biogeochemistry of Seasonally Snow-Covered Catchments* (Ed. by K. Tonnessen, M. W. Williams and M. Tranter), IAHS Publ. no. 228, pp. 157-166.

Cline, D. (1997) Snow surface energy exchanges and snowmelt at a continental, midlatitude Alpine site, *Water Resour. Res., Vol. 33*, pp. 689-701.

Halberstam, I., and Schieldge, J. P. (1981) Anomalous behavior of the atmospheric surface layer over a melting snowpack, *J. Appl. Meteorol., Vol. 20*, pp. 255-265.

Imberger, J., and Patterson, J. C. (1990) *Physical Limnology*, Academic Press.

Jordan, R. (1991) A one-dimensional temperature model for a snow-cover, Spec Rep. 91-16, U. S. Army Cold Reg. Res. and Eng. Lab., Hanover, N. H.

Kattelmann, R. C. (1995) Water Movement and Ripening Processes in Snowpacks of the Sierra Nevada, Ph. D. Thesis, Dept. of Geogr., Univ. of Calif., Santa Barbara.

Kattelmann, R., and Elder, K. (1991) Hydrologic characteristics and water balance of an alpine basin in the Sierra Nevada, *Water Resour. Res., Vol. 27*, pp. 1553-1562.

Katul, G. K., and Parlange, M. B. (1992) A Penman-Brutsaert model for wet surface evaporation, *Water Resour. Res., Vol. 28*, pp. 121-126.

Kuusisto, E. (1986) The energy balance of a melting snow cover in different environments, In: *Modeling Snowmelt-Induced Processes*, IAHS Publ. no. 155, pp. 37-45.

Male, D. H., and Granger, R. J. (1979) Energy and mass fluxes at the snow surface in a prairie environment, In: Proceedings, Modeling of Snow Cover Runoff (ed. by S. C. Colbeck and M. Ray), CRREL, Hanover New Hampshire, pp. 101-124.

Marks, D., Dozier, J., and Davis, R. E. (1992) Climate and energy exchange at the snow surface in the alpine region of the Sierra Nevada, 1. Meteorological measurements and monitoring, *Water Resour. Res.*, *Vol. 28*, pp. 3029-3042.

Marks, D., and Dozier, J. (1992) Climate and energy exchange at the snow surface in the alpine region of the Sierra Nevada, 2. Snow cover energy balance, *Water Resour. Res.*, *Vol. 28*, pp. 3043-3054.

Matthes, F. E. (1934) Ablation of snowfields at high altitudes by radiant solar heat, *Trans. AGU*, *Vol. 2*, pp. 380-385.

Melack, J. M., Sickman, J. O., Leydecker, A., and Marrett, D. (1997) Comparative Analysis of High-Altitude Lakes and Catchments in the Sierra Nevada: Susceptibility to Acidification, Calif. Air Resources Board, Project A032-188.

McKay, D. C., and Thurtell, G. W. (1978) Measurements of the energy fluxes involved in the energy budget of a snow cover, *J. Appl. Meteorol.*, *Vol. 17*, pp. 339-349.

Moore, R. D. (1983) On the use of bulk aerodynamic formulae over melting snow, *Nordic Hydrology, Vol. 14*, pp. 193-206.

Morris, F. M. (1989) Turbulent transfer over snow and ice, *J. Hydrology*, *Vol. 105*, pp. 205-223.

Morton, F. I. (1983) Operational estimates of areal evapotranspiration and their significance to the science and practice of hydrology, *J. Hydrology*, *Vol. 66*, pp. 1-76.

Oke, T. R. (1987) *Boundary Layer Climates*, Routledge, New York, NY.

Parlange, M. B., and Brutsaert, W. (1989) Regional roughness of the Landes Forest and surface shear stress under neutral conditions, *Boundary Layer Meteorol.*, *Vol. 48*, pp. 69-81.

Pluss, C., and Mazzoni, R. (1994) The role of turbulent heat fluxes in the energy balance of high alpine snow cover, *Nordic Hydrology*, *Vol. 25*, pp. 25-38.

Saucer, W. J. (1955) *Principles of Meteorological Analysis*, Univ. of Chicago Press.

Sharp, R. P. (1951) Melting versus evaporation in the Sierra Nevada, California, *J. Glaciology*, *Vol. 1*, p. 583.

Received: 25 March, 1998
Revised: 14 January, 1999
Accepted: 21 January, 1999

Address:
Dept. of Ecology, Evolution and Marine Biology, and
the Institute for Computational Earth System Science,
University of California,
Santa Barbara, CA 93106,
U.S.A.
Al Leydecker
Email: al@icess.ucsb.edu